Rapid and efficient magnetization of mesenchymal stem cells by dendrimer-functionalized magnetic nanoparticles

Nunzia Di Maggio[1*], Elisa Martella[2,3*], Steve Meikle[4], Marta Columbaro[5], Enrico Lucarelli[2], Matteo Santin[4‡] and Andrea Banfi[1‡]

[1]Cell and Gene Therapy, Department of Biomedicine, Basel University and Department of Surgery, Basel University Hospital, Basel, Switzerland

[2]Osteoarticular Regeneration Laboratory, Rizzoli Orthopaedic Institute, Bologna, Italy

[3]Department of Biomedical and Neuromotor Sciences (DIBINEM), University of Bologna, Italy

[4]BrightSTAR, Brighton Centre for Regenerative Medicine, University of Brighton, UK

[5]Musculoskeletal Cell Biology Laboratory, Rizzoli Orthopaedic Institute, Bologna, Italy

* These authors contributed equally

‡ These authors contributed equally

Running head: Rapid magnetization of stem cells by dendrimers

Send correspondence to:

Dr. Andrea Banfi, Cell and Gene Therapy, Department of Biomedicine, Basel University Hospital, Hebelstrasse 20, 4031 Basel (Switzerland); e-mail: andrea.banfi@usb.ch

or to:

Prof. Matteo Santin, Brighton Studies in Tissue-mimicry and Aided Regeneration (BrightSTAR), Brighton Centre for Regenerative Medicine, University of Brighton, Huxley Building, Lewes Road, Brighton, BN2 4GJ (UK); e-mail: m.santin@brighton.ac.uk

ABSTRACT

Aims Rapid and efficient magnetization of human bone marrow stromal cells (BMSC) through functionalized magnetic nanoparticles (MNP).

Methods MNP were functionalized with poly(epsilon-lysine) dendrons exposing carboxybetaine residue (CB-MNP) to enhance binding to the cellular glycocalix. BMSC were incubated with CB-MNP or non-functionalized PAA-MNP for 5-30 minutes in suspension.

Results CB-MNP functionalisation increased the magnetization efficiency by 3-fold. Remarkably, 66% of cells were magnetized after only 5 minutes and the maximum efficiency of >80% was reached by 15 minutes. BMSC viability, proliferation and differentiation were not impaired: actually, adipogenic and osteogenic differentiation were even improved.

Conclusions Carboxybetaine-dendron functionalization ensured rapid and efficient BMSC magnetization and allowed innovative suspension labelling, with a potential for bypassing adhesion culture of progenitors for regenerative medicine.

KEYWORDS: Dendrimers; Nanoparticles; Stem cells

INTRODUCTION

Cell-based therapies aim at regenerating fully-functional tissues damaged by surgery, trauma or disease, where their spontaneous repair is insufficient or leads to non-physiological healing [1]. Tissue engineering, based on the combination of suitable progenitor cells with biocompatible scaffolding materials, is the most advocated strategy as it enables both control over cell behaviour and retention upon transplantation [2,3].

Mesenchymal stem/stromal cells (MSC) are widely accepted as the best candidates in this type of regenerative medicine approach as they are able to differentiate into the three main mesenchymal lineages reaching complete differentiation both *in vitro* and *in vivo*, particularly into cells of the musculoskeletal system [4]. Therefore, this phenotypic plasticity encourages its main therapeutic application in the regeneration of damaged bone or cartilage, where the clinical demand is not met by satisfactory surgical solutions [2,5–7]. Studies of MSC obtained from different sources show that those isolated from bone marrow (Bone Marrow Stromal Cells, BMSC) possess a greater ability to differentiate into the osteogenic lineage both *in vitro* and *in vivo* when compared to MSC derived from other tissues [8–11]. The use of MSC for bone regeneration can be optimized in a tissue engineering approach where these cells are combined with natural or synthetic matrices able to mimic the extracellular matrix of connective tissue, hence favouring the differentiation of either host migrating progenitors or transplanted cells [3,12]. In the latter case, an optimal seeding of the progenitor cells is the required first step to ensure a homogeneous regeneration of the tissue throughout the scaffold. In particular, high seeding density and uniform cell distribution through the scaffold are critical to promote homogenous tissue formation and achieve clinical success [13]. Bioreactors, including spinner flasks and perfusion bioreactors, are a very effective technology to reach this goal and can overcome the limitations of static loading of highly concentrated cell suspensions [14]. However, bioreactor-based seeding procedures require one or more days of *in vitro* culture to allow cell distribution and attachment to the scaffolds

[15]. On the other hand, it is highly desirable from a clinical point of view to develop intraoperative approaches, whereby progenitors are harvested, seeded onto the scaffold and re-implanted into the patient directly without an *in vitro* culture step; this allows the operator to minimize the negative effects of cell manipulation [16] and to reduce costs for cell expansion under GMP manufacturing conditions [17,18].

Magnetic forces capable of driving cells through the 3D scaffold mesh could provide an attractive means to achieve its rapid and homogenous seeding [19]. It has been suggested that this magnetic drive can be achieved through the coupling of cells to superparamagnetic nano-particles (MNP). MNP (from 5 to 150 nm in diameter) can be engineered to have their magnetic core coated with different polymeric materials, including dextran, polylysine, chitosan or silica [20,21]. The application of these coatings does not alter the magnetic properties of the MNP, but enhances their biocompatibility and promote their endocytosis, a step necessary to the final magnetization of the cells [22]. However, cell labelling with MNP is a slow and low-yield process often not able to guarantee levels of magnetization sufficient for cell manipulation. Indeed, published data show that it is necessary to incubate MNP *in vitro* on adherent cells for prolonged periods of time, ranging between 12 and 24 hours [23–26]. This is a limitation that currently precludes the use of magnetized cells in most biomedical applications.

This work reports a novel method based on the surface functionalization of MNP with biocompetent dendrons that significantly accelerates and improves the magnetization of human BMSC. The interaction between MNP coated by a thin layer of poly(acrylic acid) (PAA) and BMSC was achieved through the surface functionalization of the PAA coating with hyperbranched poly(epsilon-lysine) dendrons, the uppermost branching generation of which was tethered with the zwitterionic modified amino acid carboxybetaine. It was hypothesized that the high-density presentation of this highly hydrophilic amino acid could favour the interaction between the MNP and the cell surface glycocalyx, thus enhancing MNP

internalization. The significantly improved labeling efficiency of cells by functionalized MNP enabled the establishment of a novel culture-free protocol of BMSC magnetization that ensures their rapid and highly efficient magnetization in suspension, while preserving their differentiation potential, thereby enabling the possibility to bypass adhesion culture of mesenchymal progenitors.

MATERIALS AND METHODS

Dendron Synthesis

Poly (ε-lysine) dendrons of three (Gen_3K) branching generation type were synthesised on a Tenta Gel S ($-NH_2$) resin (Iris Biotech GmbH, Germany) using a previously reported 9-fluorenylmethoxycarbonyl (Fmoc) solid phase peptide method based on the sequential addition of Fmoc-protected amino acids [27]. Dendrons were designed with a cysteine as core molecule. The resin was placed inside a reaction vessel and swollen in N, N – dimethylformamide (DMF) (Fisher Scientific UK) for 15 minutes. After washing with 3 x 7 cm^3 DMF, the addition of an acid labile Rink amide linker (Iris Biotech GmbH, Germany) to the resin was undertaken via the C-terminal of the linker. The Rink amide linker was added to allow the final cleavage of the product from the resin. The exposure of N-terminal amines allowed the final assembly of the carboxybetaine molecule tethering the uppermost branching generation. The obtained dendrimer [C-Gen3K$(CB)_{16}$] was allowed to stand for 30 minutes for a final deprotection step in 20 % $^{v}/_{v}$ piperidine (Sigma Aldrich Co. Ltd, UK) in DMF and washed with 3 x 7 cm^3 DMF. The contents of the reaction vessel were then washed with 40 cm^3 dichloromethane (Fisher Scientific, UK), methanol (Fisher Scientific, UK) and diethylether (Fisher Scientific, UK). Then, the product of synthesis was dried and weighed prior to be cleaved from the resin. After three hours incubation, the solution was passed down a Pasteur pipette filled with 1 cm of a glass wool and the crude peptide was collected in a tube containing 20 cm^3 of chilled diethylether. The solution was then centrifuged (Denley BS400) at 3500 rpm for 5 minutes to collect the dendron. The diethylether was then carefully decanted from the tube and fresh diethylether 20 cm^3 was added and the sample was vortexed to disrupt the peptide pellet. The centrifugation procedure was then repeated twice more and the diethylether was subsequently decanted off. The reaction product was then freeze dried (Christ Alpha2-4), dissolved in ethanol and filtered through a syringe filter with a pore diameter of 0.22 μm (GE Healthcare Amersham, UK) prior to characterisation.

Dendron Characterisation

Once synthesised the dendron was characterised by analytical HPLC to determine purity and further purified by further by preparative HPLC. microTOF mass spectrometry was used to characterize the dendron. The crude peptide was separated by a standard analytical HPLC method (Waters^{TM} 717 plus Autosampler) performed on a hydrophobic RP 18 column (150x4.60 mm, Luna 3u C18 100A, Phenomenex) at 25° C (Column chiller Model 7955, Jones Chromatography). The mobile phase consisted of a stepwise gradient of two solvent systems (Solvent A deionised water with 0.1% v/v TFA, Solvent B acetonitrile with 0.1% v/v TFA). Chromatograms were recorded on UV detector (SPO-6A, Shimadzu) and analysed by HPLC software, Total Chrom-TC Navigator.

Attachment of Dendron to Fe3O4@PAA MNP

Fe_3O_4@PAA super magnetic nanoparticles were produced by Nanogap S.L. (Santiago de Compostela, Spain) as previously described [23]. Fe_3O_4@PAA (13 mg) were washed three times with 20 ml of ethanol. A 20 ml volume of 0.1 M MES buffer containing 38 mg EDC and 6 mg NHS was added, the solution was vortexed for 30 seconds and then placed in the shaking incubation for 30 minutes. L-cysteine (25 mg, 0.2 mM) was added and the mixture was shaken for 1 h. The MES buffer was removed and the beads washed three times with ethanol. The beads were then split into two tubes. To conjugate the dendrimers to the cysteine via a disulfide bridge, 10 ml of 8 M urea containing 3% w/v hydrogen peroxide were added along with (i) 5.3 mg, 1 µmole dendrimer. The tubes were then returned to the shaking incubator for 30 minutes. Non functionalized and dendron-functionalized PAA-MNP [PAA-MNP-C-Gen3K$(CB)_{16}$] were characterized by FTIR to show the successful biofunctionalization of the MNP. Each sample was examined using FTIR-ATR (Nicolet) 64 scans, 1 cm^{-1} resolution in the range 4000-650 cm^{-1}. All samples were washed three times in

ethanol for disinfection, dried by evaporation under sterile conditions and stored at 4° C until used.

BMSC culture

Bone marrow (BM) aspirates were obtained from four healthy donors of similar age (35, 36, 37 and 44 years old, 3 male and 1 female), during routine orthopaedic surgical procedures, in accordance with the local ethical committee (Ref. Nr. EK:78/07) and after informed consent. Bone marrow nucleated cells (BMNC) were isolated as previously described [28]. Briefly, BM was diluted 1:10 with phosphate-buffered saline (PBS) (Sigma-Aldrich, Saint Louis, MO) and nucleated cells were counted after staining with crystal violet solution 0.01% (Sigma Aldrich, Saint Louis, MO). BMNC were then seeded in tissue culture dishes at a density of $1x10^5$ cells/cm^2.

BMSC were expanded in complete medium (CM), consisting of α-MEM supplemented with 10% foetal bovine serum (FBS), 1% HEPES, 1% Sodium pyruvate and 1% Penicillin-Streptomycin-Glutamin (100x) solutions (all from Gibco, Life Technologies, Switzerland), and conditioned with 5 ng/ml FGF-2 (R&D systems, Minneapolis, MN) [29]. At a sub-confluent density of about 80%, cells were washed once with PBS, detached using 0.05% trypsin (Gibco) for 5 min at 37° C and counted to assess the number of population doublings. BMSC were then plated at a density of $3x10^3$ cells/cm^2 for further *in vitro* expansion in tissue culture dishes (TPP, Trasadingen ,Switzerland).

Flow cytometry

For phenotypic characterization of BMSC, cells were incubated for 20 minutes on ice, in PBS with 5% BSA. The antibodies used were: CD90-FITC, CD73-PE, CD45-FITC, IgG1-FITC, IgG1-PE (all from Becton, Dickinson and Company, Franklin Lakes, NJ) and CD105-FITC (Serotec Ltd. Oxford, UK). All the antibodies were used at a dilution of 1:50, except

CD105-FITC, which was used at 1:20. Data were acquired with a FACSCalibur flow cytometer (BD Biosciences) and analyzed by using FlowJo software (Tree Star, Ashland, OR, USA).

Labeling of BMSC with CB-MNP

In order to obtain a starting reference concentration of 7 mg/ml, 3.5 mg of CB-MNP and PAA-MNP magnetic nanoparticles were resuspended in 500 µl of 100% ethanol. To improve bead disaggregation, microcentrifuge tubes were placed in an ultrasonicating bath for 1 hour, vortexing them every 10 minutes to allow for complete resuspension. In a 50 ml tube, BMSC were resuspended in an appropriate volume of CM to reach a final concentration of $4x10^4$ cells/ml. Three different concentrations of both magnetic nano-particles were tested, respectively: low = 7.2 µg/10^4 cells, medium = 14.4 µg/10^4 cells and high = 28.8 µg/10^4 cells. The magnetic nanoparticles were added to cell suspension and incubated at 37°C, 5% CO_2 on an orbital shaker (100 rpm) for 5, 15 min or 30 minutes (2 replicates/donor for 3 independent donors, n=6 for each condition).

At the end of the incubation, efficiently labelled MSC were separated by application of an external magnet on the side of the vertically held tube for 10 minutes, so that magnetic force would not coincide with gravity. After labeling the non-magnetized cells were collected in a new tube to be separated from the magnetized ones. Both cell subpopulations were centrifuged for 5 minutes at 1500 rpm and counted to determine the percentage of magnetized cells. Magnetized cells were resuspended in CM and seeded in tissue culture dishes for further analyses.

Cytotoxicity assay

In order to determine whether magnetic labeling was toxic, labeled cells were seeded in six-well plates (TPP) at a density of $6x10^5$ cells/cm^2 (3 wells/donor for 2 independent donors,

n=6 for each condition). After 1, 2 and 3 days medium was discarded and cells were incubated with Propidium Iodide (PI) solution (diluted 1:20 in CM; Sigma Aldrich) for 20 minutes at 37° C, 5% CO_2. At the end of the incubation, fresh medium was added and images of ten random fields for condition were acquired (Olympus IX50 con camera Color View Olympus) both in brightfield and using a red fluorescent filter. Live and PI-positive cells were counted and the results were expressed as the percentage of viable cells.

In vitro proliferation

After labeling, magnetized BMSC were seeded in T75 tissue culture flasks at the density of $3x10^5$ cell/cm^2 (2 flasks/donor for 3 independent donors, n=6 for each condition) and they were expanded for two further passages. The number of population doublings was calculated at each passage according to formula: $Log_2 (N/ N_0)/t$, where N is the number of cells obtained after x days, N_0 is the number of cells seeded at time 0, and t is the time between two passages.

Trasmission Electron microscopy

Labeled BMSC were seeded on glass coverslips for six hours and then the samples were fixed with 2.5% glutaraldehyde in 0.1 M cacodylate buffer pH 7.6 for 1 h at room temperature. After post-fixation with 1% OsO4 in cacodylate buffer for 1 h, cells were dehydrated in an ethanol series and embedded in Epon resin. Ultrathin sections stained with uranyl acetate and lead citrate were observed with a Jeol Jem-1011 transmission electron microscope (Jeol Jem, USA). Two hundred nuclei were examined for each sample. In order to quantify the number and the size of magnetic nanoparticle aggregates that had been internalized by each cell, the area occupied by magnetic nanoparticles was identified using region of interests (ROI) tool and successively calculated by the software (Nis D 4.10 software from Nikon, Amsterdam, Netherlands).

Confocal scanning microscopy

After labeling, BMSC were seeded on glass coverslips and allowed to adhere overnight. After three washes in PBS, the cell monolayer was fixed with 4% PFA at room temperature (RT) for 20 min. Non-specific sites were blocked with 1% Bovine Serum Albumin (BSA, Sigma Aldrich) in PBS for 30 minutes at RT. Fixed cells were incubated with a primary antibody against CD90 (clone 5E10, Abcam, 1:50 in blocking solution) overnight at 4° C in humid chamber. After three washes in PBS for 5 minutes, Cy3-conjugated anti-mouse IgG (1:100 in PBS 1X Sigma-Aldrich) secondary antibody was added and incubated for 1 hour at RT. After three washes in PBS, coverslips were mounted in Fluoromount-G solution and imaged. A confocal laser scanning microscopy analysis of intracellular localization of MNP was performed using a Nikon TiE microscope equipped with a fully automated A1 confocal laser which incorporates the resonant scanner with a resonance frequency of 7.8 kHz allowing high-speed imaging (A1R, Nikon, Amsterdam, Netherlands). Reflection and fluorescence modes were applied sequentially for detection of MNP and CD90 signal, respectively. In reflection mode, the sample was excited with a 488 nm laser: light reflected by the MNP passed through a beam splitter (20/80), was reflected by a 450/50 nm filter and was detected by a photomultiplier. The CD90 signal was instead detected by fluorescence emission of the Cy-3 fluorophore after excitation by 561 nm laser light. Z-stack acquisition (0,22 nm and 0,13 nm single step respectively for PAA-MNP and CB-MNP) was performed and the confocal pinhole was set to 1.2 Airy disk and a 60X Plan-Apochromatic PhN2 1.4NA objective lens was used. Orthogonal projection was applied to evaluated MNP position in relation to cell membrane. Ten images per condition were analysed (n = 10).

In vitro Osteogenic Differentiation

Osteogenic differentiation was induced in monolayer as previously described (Jaiswal, *et al.*, 1997). Briefly labeled BMSC were seeded in 6-well plates (8 wells/donor from 2 independent donors, 4 of which used for Alizarin Red staining and 4 for calcium quantification; n=8 for each condition and assay) at a density of $3x10^5$ cells/cm^2 in α-MEM supplemented with 10% FBS until they reached confluency. Medium was then supplemented with 10 mM β-glycerophosphate, 10 nM dexamethasone and 0.1 mM L-Ascorbic acid-2-phosphate (all from Sigma) for three weeks (Osteogenic medium, OM) and changed twice per week. After 21 days of osteogenic induction, the cell layer was washed once with PBS, fixed with 4% formalin for 10 min at room temperature and rinsed extensively with distill H_2O. Cells layer was incubated with 2% Alizarin red (AR-S Sigma Aldrich) solution for 10 min at room temperature and when the solution was removed plates were washed twice with 100% ethanol and images were acquired using a phase-contrast microscope (Olympus IX50 with a Color View camera). The total calcium amount was quantified using the Calcium quantification kit CA-590 (RANDOX, Crumlin, United Kindom). Briefly, at the end of osteogenic induction the cell monolayer was washed twice with PBS and scratched adding 0.5 N HCl in each well. Cell lysates were transferred in microcentrifuge tubes and were shaken for 3 hours at 4° C on an orbital shaker. At the end of the incubation the solution was spun at 1000 rpm for 5 minutes. The supernatant was collected in a new tube and stored at -20° C until the analysis. The working solution was prepared adding equal parts of the two components R1 (calcium buffer) and R2 (Calcium chromogen). In a 96-well plate, 5 µl of cell lysate were added to 195 µl of working solution and absorbance was read at 575 nm. A standard curve was prepared using Calcium/Phosphate at 5 different concentrations between 0-100 µg/ml.

In vitro Adipogenic Differentiation

Adipogenic differentiation was induced as previously described [31]. Briefly, cells were seeded in 6-well plates at a density of $3x10^5$ cells/cm^2 (4 wells/donor from 2 independent donors, n=8 for each condition) and cultured in CM until confluence. The medium was then supplemented with 10 µg/ml Insulin, 1 µM Dexamethasone, 100 µM indomethacin and 500 µM 3-isobutyl-1-methyl-xanthine (adipogenic induction medium, AIM) for 72 hours and subsequently combined with 10 µg/ml insulin (all from Sigma Aldrich) (adipogenic maintenance medium, AMM) for 24 hours. The 96-hour treatment cycle was repeated four times. At the end of adipogenic induction, the cell monolayer was washed with PBS, fixed in 4% formalin for 10 minutes and stained with three volumes of Oil Red O (Sigma Aldrich) in 0.3% v/v isopropanol and two volumes of H_2O for 15 minutes at room temperature. Representative micrographs were acquired using a brightfield microscope (Olympus IX50 with a Color View camera). Oil Red O, contained in lipid droplets, was then solubilized with 100% isopropanol and the optical density was measured with a spectrophotometer at 500 nm [32].

Statistical Analysis

Results are expressed as mean ± SEM. Before statistical testing, Kolmogorov-Smirnov test was performed on all data sets to assess normal distribution. The data reported in Figure 6 did not satisfy the normality test and were therefore analyzed with the non-parametric Kruskal-Wallis test for multiple comparisons and Dunn's post-hoc test. All other data sets passed the normality test and were therefore analysed using 1-way ANOVA and Bonferroni's multiple-comparison test as a post-test. Results were considered to be statistically significant at p values < 0.05 (* = $p < 0.05$, ** = $p < 0.01$, *** = $p < 0.001$). The data, including median value with range or mean value with SEM, were processed with GraphPad Prism 5 Software (GraphPad; San Diego, CA, USA).

RESULTS

Dendrimer synthesis and MNP functionalization

Mass spectrometry confirmed the successful synthesis of dendrons with peaks corresponding to various charged peptides, all multiples of the theoretical molecular weight (M): 3644.6. These corresponding peaks were: M^{12+} *m/z* 303.84, M^{9+} *m/z* 405.11, $(M+11H)^{11+}$ *m/z* 332.41, $(M+9H)^{9+}$ *m/z* 406.12, $(M + 4H)^{4+}$ *m/z* 912.52.

The final yield of the reaction was 50 mg of dendrimers from an initial 100 mg of solid-phase resin, with a purity of 63%, corresponding to a single HPLC peak eluted at 14 min.

Figure 1A summarizes the structure of MNP functionalized with the hyperbrached poly(epsilon lysine) dendrons. Fe_3O_4 magnetic nanoparticles were coated with a thin layer of polyacrilic acid (PAA-MNP) and successively functionalized with dendrons of poly(epsilon lysine) to yield PAA-MNP-C-Gen3K$(CB)_{16}$, which will be referred to as CB-MNP in the rest of the manuscript for simplicity. PAA-MNP and CB-MNP were characterized for Fourier Transform Infrared Spectroscopy (FTIR). Functionalized CB-MNP showed the typical amine I and amine II peaks of the dendrons (Figure 1B, red arrows) in the region comprised between 1400 cm-1 and 1600 cm-1, which were instead not found in the non-modified PAA-MNP (Figure 1C). The size of non-functionalized PAA-MNP nanoparticles was 18.46 nm with a zeta potential of –45.6 mV and the functionalization with dendrons led to an increase in the measured hydrodynamic radius to 33.37 nm and a zeta potential of –25.6 mV (Meikle et al, manuscript submitted).

Dose-dependent cytotoxicity and labelling efficiency of functionalized CB-MNP

Phenotypic characterization of isolated BMSC confirmed that the populations were almost uniformly positive for mesenchymal markers (CD105 = 97.8±0.8%, CD90 = 81.3±8.0% and CD73 = 98.9±0.4%) whereas the presence of leukocytes was extremely infrequent (CD45 = 0.5±0.2%), in agreement with previous results [28,33,34].

In order to minimize manipulation of isolated BMSC, we developed a protocol to rapidly label cells in suspension rather than in adhesion culture (Figure 2A). Cells were re-suspended in a 50-ml tube in complete culture medium, in order to avoid serum deprivation during the labelling procedure, at a concentration of $4x10^4$ cells/ml and MNP were added (step1). Labelling took place during a 30-minute incubation on an orbital shaker to avoid sedimentation of cells and MNP (step 2). Efficiently labelled MSC were then separated by application of an external magnet on the side of the vertically held tube, so that magnetic force would not coincide with gravity (step 3), and isolated cells were plated on tissue culture dishes for further analyses (step 4).

To investigate which CB-MNP concentration could preserve cell viability while bestowing a magnetization level sufficient for manipulation, increasing concentrations of CB-MNP were tested with a fixed number of target cells. A starting concentration of 14.4 µg CB-MNP/10^4 cells (medium concentration) was calculated from published experiments performed using a different protocol on adherent cells [35], transforming the amount reported there in µg of MNP/10^4 cells, to be incubated in suspension labeling in a standard volume. Starting from this reference dose, which was shown to produce efficient magnetization with multi-hour incubations on adherent cells, 2-fold lower and higher concentrations were included (low = 7.2 µg CB-MNP/10^4 cells and high = 28.8 µg CB-MNP/10^4 cells). After magnetic separation, labelling efficiency was measured by counting the cells retained by the magnet compared to the total number before the incubation. After 30 minutes of incubation with CB-MNP, >80% of the cells were successfully magnetized at all three tested concentrations (low=82.7±7.9%, medium=85.5±4.0%, high=85.0±2.8%, p not significant for all comparisons), indicating that the labelling conditions were saturating in this range. Cells were then allowed to adhere to plastic at 37°C for 24 hours. Labelling was clearly visible under transmitted light and it did not affect the morphology and the adherence properties of the cells. CB-MNP formed macroscopic aggregates, which appeared mainly localized on the cell membrane at this stage

(Figure 2B, red arrows). Interestingly, CB-MNP that were not associated with cells could be seen to form much smaller aggregates (Figure 2C, white arrows), suggesting a reduced propensity for spontaneous aggregation. A cytotoxicity test was performed 24, 48 and 72 hours after labelling. Viability was always close to 99% with all CB-MNP doses at all time-points and did not differ from that of unlabelled control MSC (Figure 2D). Taken together, these results indicate that a 4-fold range of CB-MNP doses allowed rapid and efficient magnetization of human BMSC without signs of cytotoxicity.

Effect of magnetic labeling with CB-MNP on MSC proliferation

After labelling with the different CB-MNP doses and magnetic separation, BMSC were plated at low density to measure the possible effects of CB-MNP on active cell proliferation. Before reaching confluence the cells were detached and counted (Passage 1), re-plated at low density and counted again after a further passage to determine the number of population doublings (Passage 2). Proliferation was slower at the second passage compared to the first, as primary BMSC are well-known to gradually reduce their doubling time over the first few passages in culture [29,36]. However, no significant differences were found in the number of doublings per day between the different CB-MNP doses and in comparison with control conditions, at both passages (Figure 3), indicating that CB-MNP labelling did not interfere with BMSC adhesion and proliferation capacity.

Adipogenic and osteogenic differentiation potential of BMSC after CB-MNP labelling

To determine the effects of labelling with the different CB-MNP doses on BMSC differentiation potential, after magnetic separation cells were expanded on tissue culture plastic for one passage and then treated with adipogenic or osteogenic differentiation-inducing factors.

Under adipogenic conditions, both control and CB-MNP-labeled MSC generated mature adipocytes (Figure 4A), characterized by mature lipid vacuoles revealed by Oil Red O staining. Quantification of the amount of lipid deposition after Oil Red O extraction showed that differentiation of cells labelled with all CB-MNP concentrations was improved by about 30% compared to that of unlabelled control BMSC (Figure 4B).

Following osteogenic stimulation, BMSC differentiated efficiently under all conditions, as evidenced by the production of Alizarin Red-positive calcium deposits *in vitro* (Figure 5A). Since Alizarin Red staining provides only semi-quantitative results, osteogenic differentiation was precisely measured by biochemical quantification of the deposited calcium after lysis of the cell layers, revealing that labelling with all three doses of CB-MNP significantly increased osteogenic differentiation by more than 2-fold compared to control naïve cells (Figure 5B).

Rapid magnetization of BMSC by CB-MNP

In any biomedical or biotechnological application involving the use of MSC, it is desirable to minimize the duration of the labelling procedure without compromising the efficiency of the whole operation. Therefore, in order to determine the minimum necessary duration of labelling, BMSC were incubated with the lowest of the three previously tested doses of CB-MNP (7.2 µg/10^4 cells), since this already ensured the maximum labelling efficiency and the percentage of magnetized cells was measured after incubation for 5, 15 and 30 minutes and compared with the same dose of non-functionalized PAA-MNP to determine the effect of the dendron C-Gen3K$(CB)_{16}$. As shown in Figure 6, labelling with PAA-MNP led to a magnetization efficiency of 27.9±10.9% after 5 minutes of incubation, which did not improve with longer labelling times up to 30 minutes (21.3±12.1% and 23.4±6.8% for 15 and 30 minutes respectively, p=n.s.). However, CB-MNP could efficiently magnetize already 66.2±14.4% of cells with only 5 minutes of incubation and labelling efficiency increased to 79.0±6.7% and 83.7±6.8% after 15 and 30 minutes respectively. Therefore, functionalization

with C-Gen3K$(CB)_{16}$ led to an increase of 2.4-fold in the BMSC magnetization efficiency by PAA-MNP ($p<0.001$) with an incubation time as rapid as only 5 minute.

Effect of CB functionalization on PAA-MNP internalization

In order to determine the fate of MNP after cell labelling, MSC were incubated with the lowest dose (7.2 µg/10^4 cells) of CB-MNP or PAA-MNP for 5 and 30 minutes and the localization of MNP was analysed by confocal microscopy and transmission electron microscopy (TEM) after adhesion to coverslips, washing of unbound particles and fixation (overnight for confocal analysis and 6 hours for TEM). For confocal microscopy, the cell membrane was marked by immunostaining for the BMSC surface marker CD90 (in red in Figure 7), while MNP were visualized in the green channel taking advantage of the intrinsic property of iron-containing MNP to reflect fluorescent light. Both types of MNP could be clearly seen on the internal side of the BMSC cell membrane in the orthogonal projections of confocal z-stacks. However, while rarely some PAA-MNP clusters could be observed also attached to the cell surface outside the membrane, possibly in the act of being internalized (Figure 7B), functionalized CB-MNP appeared almost exclusively internalized (Figure 7A).

To more rigorously determine how CB functionalization may affect the cell binding and internalization processes, samples were analysed by TEM (Figure 8). After incubation for either 5 or 30 minutes, both kinds of MNP were visible inside cytoplasmic vacuoles as well as in extracellular aggregates (arrowheads and arrows, respectively, in Figure 8A-E). However, in agreement with the confocal results, cells treated with CB-MNP showed smaller and less dense extracellular aggregates than those labelled with non-functionalized PAA-MNP. The vacuoles containing MNP aggregates were identified as early endosomes because of their electron-clear inner volume. Apart from the increased number of vacuoles, cells labelled with both kinds of MNP did not show any ultrastructural signs of cytotoxicity, as the morphology of the nucleus, mitochondria, Golgi apparatus and endoplasmic reticulum was normal and

similar to that of unlabelled control BMSC. The size and the number of intracellular MNP aggregates were quantified. As shown in Figure 8F, the size of internalized aggregates was quite variable, but on average it was similar between CB- and PAA-MNP after 5-minute incubation. However, aggregates of non-functionalized PAA-MNP became significantly larger after 30 minutes of incubation, whereas those of functionalized CB-MNP remained smaller. Further, labelling with CB-MNP led to a much greater number of internalized aggregates per microscopic field than non-functionalized PAA-MNP after incubation for both 5 and 30 minutes (3- and 6-fold more, respectively; Figure 8G). Taken together, these data suggest that carboxybetaine dendron functionalization significantly improved the efficiency of MNP adhesion to cell membrane and their subsequent internalization in the form of many small aggregates.

DISCUSSION

The present work describes a novel approach for the magnetization of multipotent mesenchymal progenitors based on the combination of: a) superparamagnetic nanoparticles functionalized with a hyperbranched dendron coating, exposing a highly hydrophilic carboxybetaine residue and designed for efficient interaction with the glycocalyx on cell membranes; and b) an optimized protocol for cell labelling in suspension, avoiding the step of adhesion culture. The combination of these two elements enabled the rapid (15 minutes) and efficient (>80%) magnetization of primary human BMSC with no impairment of their *in vitro* viability and proliferation, while their differentiation potential was even improved.

Magnetization of cells has been long considered as a suitable approach towards their separation, particularly in the field of cytofluorimetry. Cell sorting is achieved by the coupling of micron-size magnetic beads to antibodies that are able to bind specific cell surface molecules and separate the expressing cells from a heterogeneous sample through magnetic forces [37]. However, such approach is not suitable for other biotechnological and biomedical applications where, for example, magnetic forces can be used to manipulate heterogeneous progenitor populations, whose surface marker composition is only partially known, such as in tissue engineering/regenerative medicine applications. Therefore, the availability of super-paramagnetic particles of nanoscale size that can be internalized by most cells and that are activated only in the presence of a magnetic field have opened new avenues for the exploitation of magnetism in a number of biotechnological and biomedical applications. This new technological approach has also expanded the possibilities for non-invasive analysis of progenitor fate after their *in vivo* delivery, such as by magnetic resonance imaging (MRI) [38]. While MNP internalization enables the magnetization of any type of cells, concerns still remain about their potential cytotoxic and genotoxic effects. Towards this end, the coating of MNP with biocompatible materials has been proposed; these mainly include synthetic and natural polymers. However, the selection of these polymers has been rather based on the

demonstration of their biocompatibility in other applications and no reported study has been based on an *ad hoc* design of coatings where the polymer can be exploited to enhance not only the MNP biocompatibility, but also their internalization process.

In this study a unique functionalization approach has been designed that capitalises on the availability of highly homogeneous MNP coated with a 2-nm layer of poly(acrylic acid) [39]. The presence of the exposed carboxylic groups of the polymer at the surface of this type of MNP was exploited to covalently graft a novel class of hyperbranched poly(epsilon-lysine) peptides. These peptides, called dendrons, present sixteen uppermost molecular branches, all functionalised with carboxybetaine, a highly hydrophilic amino acid derivative [40]. The successful synthesis of a highly purified dendron was proven both by the single HPLC elution peak released at 14min and by the mass spectrometry showing peaks matching the multiples of the theoretical molecular weight of the dendron.

As expected, the thin poly(acrylic acid) coating of the MNP could not be detected by FTIR as its thickness was below the sensitivity limit of the instrument. The weak, near-to-background footprint of the branched peptide could be however detected when dendron-functionalised MNP were analysed. In particular, the wavelength range between 1000 and 1600 cm-1 showed at least 4 peaks that can be attributed to the primary and secondary amines present both in the poly(epsilon lysine) dendron core and in the terminal carboxybetaine [41]. These results were also corroborated by the presence of a large peak in the region ranging between 3000 and 3500 cm-1 that can be attributed to both the presence of amino groups and hydroxylic groups of water molecules bound by the highly hydrophilic carboxybetaine when exposed to air humidity [40]. The increased hydrophilicity of functionalized CB-MNP was also confirmed by work published elsewhere showing that the measured hydrodynamic radius increased from 18.46 nm to 33.37 nm after functionalization with dendrons (Meikle et al, manuscript submitted).

The cytotoxicity assay showed that the internalization of dendron-functionalized magnetic nanoparticles did not induce any apoptotic or necrotic effect, with excellent cytocompatibility (99% viability). The lack of toxicity was further corroborated by the TEM analysis, showing no alteration of the cell ultrastructure compared to the controls, and by the analysis of proliferation, showing similar population doublings between the magnetised cells and the controls. These results are in agreement with those reported by Wang et al. showing that functionalisation with carboxybetaine could greatly reduce the cytotoxicity of poly(amido amine) (PAMAM) dendrimers [42]. It should be noticed that cytocompatibility of CB-MNP was not decreased despite the fact that dendron functionalization greatly increased the labelling efficiency and the amount of nanoparticles that were internalized by each cell (Fig. 8F-G). The amounts of nanoparticles used in this study align with the literature [35] and it should be underlined that these doses could efficiently achieve levels of cell magnetization suitable for biomedical applications requiring cell drive by magnetic forces, such as rapid isolation and loading onto tissue engineering scaffolds: in fact, we analysed only the cells that could be separated by an external magnet against the force of gravity, so that insufficiently labelled cells would be eliminated. Further, labelling efficiency was similar across an 8-fold range of CB-MNP doses, despite a very short incubation time of 30 minutes, indicating that even lower doses could be investigated in order to maximize safety in future *in vivo* studies. The lack of any obvious adverse effect was corroborated by the analysis of BMSC proliferation that showed the typical, progressive increase in doubling time upon 2 passages [36], but with no difference in comparison with control non-labelled BMSC.

It was interesting to observe that both adipogenic and osteogenic *in vitro* differentiation were significantly enhanced in CB-MNP-labelled cells in comparison with non-magnetized control BMSC. Although it is not easy to postulate what could be the reason for this effect, it is possible to speculate about a possible mechanism. In fact, CB-MNP treatment caused labelled cells to more easily assemble in aggregates that required more forceful disruption for

e.g. cell counting and, since *in vitro* differentiation of BMSC is favoured by close cell-to-cell contact, the formation of such multicellular clusters could enhance the degree of BMSC differentiation, even when seeded at the same initial density.

The coupling of MNP with dendrons specifically designed to enhance interactions with the cell glycocalyx led to a significant increase in the efficiency of magnetization (80% vs 20%) as well as to a significant reduction of the time required, with 60% of the cells being effectively magnetized in only 5 minutes of incubation in suspension and the plateau value of 80% being reached already after 15 minutes. Apart from the greater affinity for the negatively charged glycocalix on the cell surface provided by the carboxybetaine moiety, causing more rapid and more stable association with the cell membrane and leading to a more efficient binding and internalization, another property of dendron functionalization may contribute to explaining these results. In fact, a comparative analysis showed that, although both types of MNP could form aggregates of similar sizes, dendron-functionalised MNP within aggregates were less densely packed (see high-magnification right panels in Figure 8B). Dynamic light scattering data published elsewhere have shown that the functionalisation of the surface with dendrons improves their polydispersity index (Meikle et al., manuscript submitted). This would lead to the formation of more aggregates containing less MNP for equivalent total doses, which is expected to increase the collective surface area of the aggregates, hence favouring its interaction with the cell surface. TEM showed that this process was not accompanied by the formation of a clathrin layer around the invagination areas of the plasmalemma (Figure 8) thus suggesting that for both types of MNP internalization was driven by macropinocitosis [43]. Such a mechanisms of internalization would emphasise the important role played by the glycocalyx in the early interaction of the MNP.

Primary human BMSC are widely investigated in regenerative medicine, both in pre-clinical research and in clinical trials, because of their recognized potential for differentiation in multiple mesenchymal lineages, as well as favourable immunomodulatory properties and

paracrine effects that can stimulate endogenous repair mechanisms [44]. However, their stem cell properties are easily lost during culture and their ability to regenerate tissue *in vivo* is rapidly jeopardized by *in vitro* expansion [28,29,36]. Therefore, it is desirable to minimize *in vitro* progenitor manipulation before *in vivo* delivery in order to maximize their therapeutic benefit. To this end, the intraoperative production of tissue-engineered grafts, i.e. the isolation of multipotent progenitors from a patient, their seeding on an appropriate scaffolding material and their re-implantation in a single-step procedure directly in the operating room, is an actively pursued strategy [45,46]. Magnetic scaffolds have been recently developed [47,48] and indeed magnetization can be exploited to rapidly and consistently drive cells prior to their transplantation. As a perspective in this direction, which should be further investigated in future experiments, the results we presented here offer a potential strategy for intraoperative magnetic labelling of BMSC without the need for plastic adhesion culture.

CONCLUSIONS

The present study shows how the surface functionalization of poly(acrylic acid)-coated MNP with a highly branched poly(epsilon-lysine) dendrimer can increase the magnetization of human BMSC in a short time when cells are in suspension. The design of the dendron allowed the high-density exposure of a highly hydrophylic moiety (carboxybetaine) to the MNP surface that is likely to favour the interaction with the cell glycocalyx. While cytotoxicity, proliferation and differentiation tests showed no significant adverse effects of dendron-functionalised MNP, the presence of the dendron showed a clear improvement in the magnetisation process of the cells when in suspension and ultrastructural studies showed how their localization in relatively low endosomes did not alter the inner organization of the cytosol. These findings provide evidences that *ad hoc* design of MNP surface functionalization can indeed ensure a safer, more reliable and more effective magnetization of human BMSC as a means of their manipulation in biotechnological and biomedical applications.

ACKNOWLEDGEMENTS

This work was supported in part by the European Union FP7 grant MAGISTER (CP-IP 214685) to AB and MS. EM was supported by Progetto FIRB-Accordi di programma 2010 COD. RBAP10447 and a Basel Cantonal University Scholarship. The authors would like to thank Dr. Santi Spartaco (CNR Bologna) for technical support with confocal imaging and Dr. Mariapia Cumani (Rizzoli Institute, Bologna) for designing the figure graphics. Magnetic nanoparticles were kindly provided by Prof. Jose Rivas (Department of Applied Physics, University of Santiago de Compostela, Spain).

REFERENCES

1. Fox IJ, Daley GQ, Goldman SA, Huard J, Kamp TJ, Trucco M. Stem cell therapy. Use of differentiated pluripotent stem cells as replacement therapy for treating disease. *Science* 345(6199), 1247391 (2014).
2. Liebergall M, Schroeder J, Mosheiff R, *et al.* Stem cell-based therapy for prevention of delayed fracture union: a randomized and prospective preliminary study. *Mol. Ther.* 21(8), 1631–8 (2013).
3. Zippel N, Schulze M, Tobiasch E. Biomaterials and mesenchymal stem cells for regenerative medicine. *Recent Pat. Biotechnol.* 4(1), 1–22 (2010).
4. Dominici M, Le Blanc K, Mueller I, *et al.* Minimal criteria for defining multipotent mesenchymal stromal cells. The International Society for Cellular Therapy position statement. *Cytotherapy* 8(4), 315–7 (2006).
5. Wakitani S, Imoto K, Yamamoto T, Saito M, Murata N, Yoneda M. Human autologous culture expanded bone marrow mesenchymal cell transplantation for repair of cartilage defects in osteoarthritic knees. *Osteoarthr. Cartil.* 10(3), 199–206 (2002).
6. Wakitani S, Nawata M, Tensho K, Okabe T, Machida H, Ohgushi H. Repair of articular cartilage defects in the patello-femoral joint with autologous bone marrow mesenchymal cell transplantation: three case reports involving nine defects in five knees. *J. Tissue Eng. Regen. Med.* 1(1), 74–79 (2007).
7. Liu Y, Wu J, Zhu Y, Han J. Therapeutic application of mesenchymal stem cells in bone and joint diseases. *Clin. Exp. Med.* 14(1), 13–24 (2014).
8. Al-Nbaheen M, Vishnubalaji R, Ali D, *et al.* Human stromal (mesenchymal) stem cells from bone marrow, adipose tissue and skin exhibit differences in molecular phenotype and differentiation potential. *Stem Cell Rev.* 9(1), 32–43 (2013).
9. Li C, Wu X, Tong J, *et al.* Comparative analysis of human mesenchymal stem cells from bone marrow and adipose tissue under xeno-free conditions for cell therapy. *Stem*

Cell Res. Ther. 6, 55 (2015).

10. Vishnubalaji R, Al-Nbaheen M, Kadalmani B, Aldahmash A, Ramesh T. Comparative investigation of the differentiation capability of bone-marrow- and adipose-derived mesenchymal stem cells by qualitative and quantitative analysis. *Cell Tissue Res.* 347(2), 419–27 (2012).

11. Squillaro T, Peluso G, Galderisi U. Clinical Trials with Mesenchymal Stem Cells: An Update. *Cell Transplant.* 1–53 (2015).

12. Panseri S, Cunha C, D'Alessandro T, *et al.* Magnetic hydroxyapatite bone substitutes to enhance tissue regeneration: evaluation in vitro using osteoblast-like cells and in vivo in a bone defect. *PLoS One* 7(6), e38710 (2012).

13. Wendt D, Marsano A, Jakob M, Heberer M, Martin I. Oscillating perfusion of cell suspensions through three-dimensional scaffolds enhances cell seeding efficiency and uniformity. *Biotechnol. Bioeng.* 84(2), 205–14 (2003).

14. Stiehler M, Bünger C, Baatrup A, Lind M, Kassem M, Mygind T. Effect of dynamic 3-D culture on proliferation, distribution, and osteogenic differentiation of human mesenchymal stem cells. *J. Biomed. Mater. Res. A* 89(1), 96–107 (2009).

15. dos Santos FF, Andrade PZ, da Silva CL, Cabral JMS. Bioreactor design for clinical-grade expansion of stem cells. *Biotechnol. J.* 8(6), 644–654 (2013).

16. Hourd P, Chandra A, Medcalf N, Williams DJ. Regulatory challenges for the manufacture and scale-out of autologous cell therapies *StemBook*. Harvard Stem Cell Institute, Cambridge, MA (2008).

17. Heathman TRJ, Nienow AW, McCall MJ, Coopman K, Kara B, Hewitt CJ. The translation of cell-based therapies: clinical landscape and manufacturing challenges. *Regen. Med.* 10(1), 49–64 (2015).

18. Trounson A, McDonald C. Stem Cell Therapies in Clinical Trials: Progress and Challenges. *Cell Stem Cell* 17(1), 11–22 (2015).

19. Bock N, Riminucci A, Dionigi C, *et al.* A novel route in bone tissue engineering: magnetic biomimetic scaffolds. *Acta Biomater.* 6(3), 786–96 (2010).

20. Babic M, Horák D, Trchová M, *et al.* Poly(L-lysine)-modified iron oxide nanoparticles for stem cell labeling. *Bioconjug. Chem.* 19(3), 740–50 (2008).

21. Yi P, Chen G, Zhang H, *et al.* Magnetic resonance imaging of Fe3O4@SiO2-labeled human mesenchymal stem cells in mice at 11.7 T. *Biomaterials* 34(12), 3010–3019 (2013).

22. Wahajuddin, Arora S. Superparamagnetic iron oxide nanoparticles: magnetic nanoplatforms as drug carriers. *Int. J. Nanomedicine* 7, 3445–71 (2012).

23. Couto D, Freitas M, Vilas-Boas V, *et al.* Interaction of polyacrylic acid coated and non-coated iron oxide nanoparticles with human neutrophils. *Toxicol. Lett.* 225(1), 57–65 (2014).

24. Mathiasen AB, Hansen L, Friis T, Thomsen C, Bhakoo K, Kastrup J. Optimal labeling dose, labeling time, and magnetic resonance imaging detection limits of ultrasmall superparamagnetic iron-oxide nanoparticle labeled mesenchymal stromal cells. *Stem Cells Int.* 2013, 353105 (2013).

25. Andreas K, Georgieva R, Ladwig M, *et al.* Highly efficient magnetic stem cell labeling

with citrate-coated superparamagnetic iron oxide nanoparticles for MRI tracking. *Biomaterials* 33(18), 4515–25 (2012).

26. Bennewitz MF, Tang KS, Markakis EA, Shapiro EM. Specific chemotaxis of magnetically labeled mesenchymal stem cells: implications for MRI of glioma. *Mol. Imaging Biol.* 14(6), 676–87 (2012).

27. Meikle ST, Perugini V, Guildford AL, Santin M. Synthesis, characterisation and in vitro anti-angiogenic potential of dendron VEGF blockers. *Macromol. Biosci.* 11(12), 1761–5 (2011).

28. Di Maggio N, Mehrkens A, Papadimitropoulos A, *et al.* Fibroblast growth factor-2 maintains a niche-dependent population of self-renewing highly potent non-adherent mesenchymal progenitors through FGFR2c. *Stem Cells* 30(7), 1455–64 (2012).

29. Bianchi G, Banfi A, Mastrogiacomo M, *et al.* Ex vivo enrichment of mesenchymal cell progenitors by fibroblast growth factor 2. *Exp. Cell Res.* 287(1), 98–105 (2003).

30. Jaiswal N, Haynesworth SE, Caplan a I, Bruder SP. Osteogenic differentiation of purified, culture-expanded human mesenchymal stem cells in vitro. *J. Cell. Biochem.* 64(2), 295–312 (1997).

31. Barbero A, Ploegert S, Heberer M, Martin I. Plasticity of clonal populations of dedifferentiated adult human articular chondrocytes. *Arthritis Rheum.* 48(5), 1315–25 (2003).

32. Donzelli E, Lucchini C, Ballarini E, *et al.* ERK1 and ERK2 are involved in recruitment and maturation of human mesenchymal stem cells induced to adipogenic differentiation. *J. Mol. Cell Biol.* 3(2), 123–31 (2011).

33. Helmrich U, Marsano A, Melly L, *et al.* Generation of human adult mesenchymal stromal/stem cells expressing defined xenogenic vascular endothelial growth factor levels by optimized transduction and flow cytometry purification. *Tissue Eng. Part C. Methods* 18(4), 283–92 (2012).

34. Helmrich U, Di Maggio N, Guven S, *et al.* Osteogenic graft vascularization and bone resorption by VEGF-expressing human mesenchymal progenitors. *Biomaterials*. 34(21), 5025–5035 (2013).

35. Jasmin, Torres ALM, Nunes HMP, *et al.* Optimized labeling of bone marrow mesenchymal cells with superparamagnetic iron oxide nanoparticles and in vivo visualization by magnetic resonance imaging. *J. Nanobiotechnology* 9(1), 4 (2011).

36. Banfi A, Muraglia A, Dozin B, Mastrogiacomo M, Cancedda R, Quarto R. Proliferation kinetics and differentiation potential of ex vivo expanded human bone marrow stromal cells: Implications for their use in cell therapy. *Exp. Hematol.* 28(6), 707–715 (2000).

37. Grutzkau A, Radbruch A. Small but mighty: how the MACS-technology based on nanosized superparamagnetic particles has helped to analyze the immune system within the last 20 years. *Cytometry. A*. 77(7), 643–647 (2010).

38. Hossain MA, Chowdhury T, Bagul A. Imaging modalities for the in vivo surveillance of mesenchymal stromal cells. *J. Tissue Eng. Regen. Med.* 9(11), 1217–1224 (2015).

39. Piñeiro-Redondo Y, Bañobre-López M, Pardiñas-Blanco I, Goya G, López-Quintela MA, Rivas J. The influence of colloidal parameters on the specific power absorption of PAA-coated magnetite nanoparticles. *Nanoscale Res. Lett.* 6(1), 383 (2011).

40. White A, Jiang S. Local and bulk hydration of zwitterionic glycine and its analogues through molecular simulations. *J. Phys. Chem. B* 115(4), 660–7 (2011).

41. Zhou M, Smith AM, Das AK, *et al.* Self-assembled peptide-based hydrogels as scaffolds for anchorage-dependent cells. *Biomaterials* 30(13), 2523–30 (2009).

42. Wang L, Wang Z, Ma G, Lin W, Chen S. Reducing the cytotoxity of poly(amidoamine) dendrimers by modification of a single layer of carboxybetaine. *Langmuir*. 29(28), 8914–8921 (2013).

43. Lojk J, Bregar VB, Rajh M, *et al.* Cell type-specific response to high intracellular loading of polyacrylic acid-coated magnetic nanoparticles. *Int. J. Nanomedicine*. 10, 1449–1462 (2015).

44. D'souza N, Rossignoli F, Golinelli G, *et al.* Mesenchymal stem/stromal cells as a delivery platform in cell and gene therapies. *BMC Med.* 13, 186 (2015).

45. Evans CH, Palmer GD, Pascher A, *et al.* Facilitated endogenous repair: making tissue engineering simple, practical, and economical. *Tissue Eng.* 13(8), 1987–1993 (2007).

46. Mehrkens A, Saxer F, Guven S, *et al.* Intraoperative engineering of osteogenic grafts combining freshly harvested, human adipose-derived cells and physiological doses of bone morphogenetic protein-2. *Eur. Cell. Mater.* 24, 308–319 (2012).

47. Russo A, Bianchi M, Sartori M, *et al.* Magnetic forces and magnetized biomaterials provide dynamic flux information during bone regeneration. *J. Mater. Sci. Mater. Med.* 27(3), 51 (2016).

48. Yun H-M, Ahn S-J, Park K-R, *et al.* Magnetic nanocomposite scaffolds combined with static magnetic field in the stimulation of osteoblastic differentiation and bone formation. *Biomaterials*. 85, 88–98 (2016).

FIGURE LEGENDS

Figure 1. MNP design and characterization

(A) Schematic representation of PAA-MNP and CB-MNP design and production; (B-C) FTIR characterization of CB-MNP (B) and PAA-MNP (C): red arrows indicate the typical amine I and amine II peaks of the dendrons.

Figure 2. BMSC labelling with CB-MNP and dose-dependent cytotoxycity

(A) BMSC labelling procedure: cell suspensions were aliquoted in a 50mL tube with CB-MNP (STEP1); cell suspension was incubated at 37°C on an orbital shaker for different times (STEP2); magnetized cells were isolated applying an external magnetic field for 10min (STEP 3); magnetized cells were seeded on tissue culture dishes for further evaluations (STEP 4). (B-C) Representative images of CB-MNP-labeled BMSC with large amounts of nanoparticles visible on cell membranes (red arrows in B) and much smaller aggregates visible in the culture dish not associated with cells (white arrows in C). (D) Cytotoxicity was assayed 24, 48 and 72 hours after labelling with three different concentrations of CB-MNP (low = 21.6 µg/ml for 3 x 10^4 cells; medium = 43.2 µg/ml for 3 x 10^4 cells; high = 86.4 µg/mL for 3 x 10^4 cells); n=3; p=n.s. for all comparisons.

Figure 3. In vitro BMSC proliferation after labelling with CB-MNP

Proliferation speed was measured as the number of population doublings/day over 2 passages for control BMSC (not magnetized, CTRL) and for BMSC labelled with the low, medium and high concentrations of CB-MNP; n=3, p=n.s. for all comparisons.

Figure 4. In vitro adipogenic differentiation of CB-MNP-labelled BMSC

(A) Representative fields of Oil Red O staining and (B) quantification of Oil Red O staining of BMSC cultured in control (Ctrl) or adipogenic medium (Adipo), for control BMSC (not magnetized, Ctrl) and for BMSC labelled with the low, medium and high concentrations of

CB-MNP. Results are expressed as the mean ± SEM and normalized to the adipogenically differentiated control BMSC; n=3; ** $p < 0.01$ *** $p < 0.001$. Size bar = 200 µm.

Figure 5. In vitro osteogenic differentiation of CB-MNP-labelled BMSC

(A) Representative fields of Alizarin Red staining and (B) quantification of total calcium deposited of BMSC cultured in control (Ctrl) or osteogenic medium (Osteo) for control BMSC (not magnetized, Ctrl) and for BMSC labelled with the low, medium and high concentrations of CB-MNP. Results are expressed as the mean ± SEM; n=3; *** $p < 0.001$. Size bar = 200 µm.

Figure 6. CB functionalization allows fast and efficient BMSC labelling

Quantification of the percentage of labelled BMSC after incubation with CB-MNP or PAA-MNP for 5, 15 or 30 minutes. Results are expressed as mean ± SD; n=3; *** $p < 0.001$.

Figure 7. Confocal microscopy analysis of MNP cellular localization after labelling

Representative z-stack images of BMSC after 30 minutes of labelling with CB-MNP (A) or PAA-MNP (B). BMSC were stained with anti-CD90 antibody (red) that marks the cell membrane, while nanoparticles were visualized by autofluorescence in the green channel. Left panels show a 3D reconstruction of all the confocal optical sections and the white square identifies the region magnified on the orthogonal projections on the right panels; size bars = 5 µm.

Figure 8. TEM analysis of MNP internalization

(A-E) Representative transmission electron microscopy images of naïve non-magnetized BMSC (A) or after labelling with CB-MNP (B-C) or PAA-MNP (D-E) for 5 or 30 minutes; N = nucleus, Cy = cytoplasm, scale bar = 2µm. Arrows indicate extracellular MNP aggregates; arrowheads indicate nanoparticles that have been internalized in vacuoles/endosomes. The white squares identify the regions magnified on the right panels. (F) Quantification of the area occupied by PAA-MNP or CB-MNP in each intracellular vacuole after 5 or 30 minutes of

labelling. (G) Quantification of the number of intracellular vacuoles/image containing PAA-MNP or CB-MNP after 5 or 30 minutes of labelling.

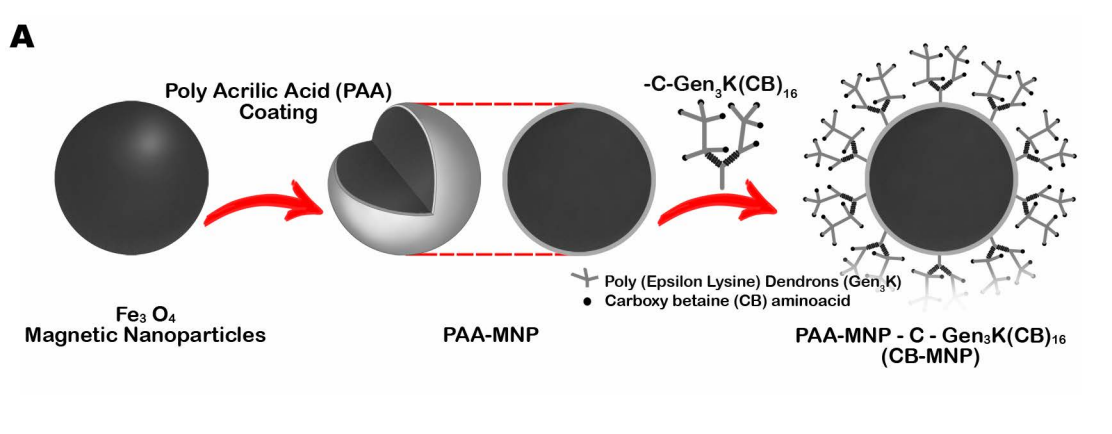
A
Poly Acrilic Acid (PAA)
Coating
-C-Gen3K(CB)16
Poly (Epsilon Lysine) Dendrons (Gen3K)
Carboxy betaine (CB) aminoacid
Fe3 O4
Magnetic Nanoparticles
PAA-MNP
PAA-MNP - C - Gen3K(CB)16
(CB-MNP)

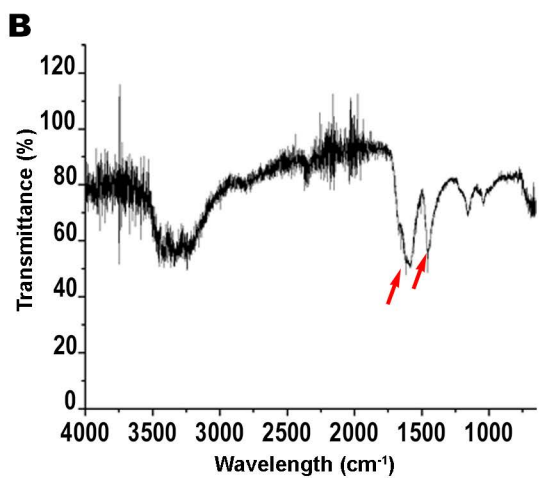
B
Transmittance (%)
120
100
80
60
40
20
0
4000 3500 3000 2500 2000 1500 1000
Wavelength (cm-1)

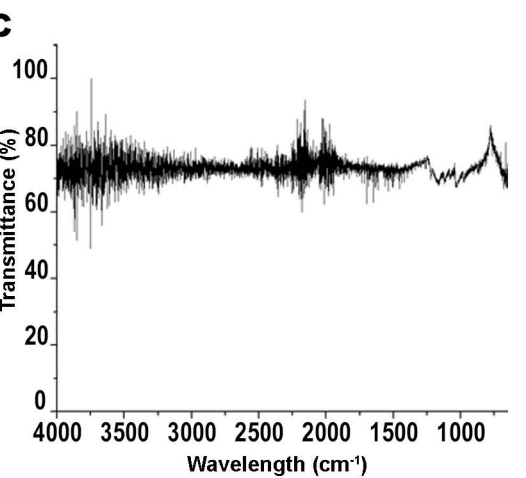
C
Transmittance (%)
100
80
60
40
20
0
4000 3500 3000 2500 2000 1500 1000
Wavelength (cm-1)

Figure 1

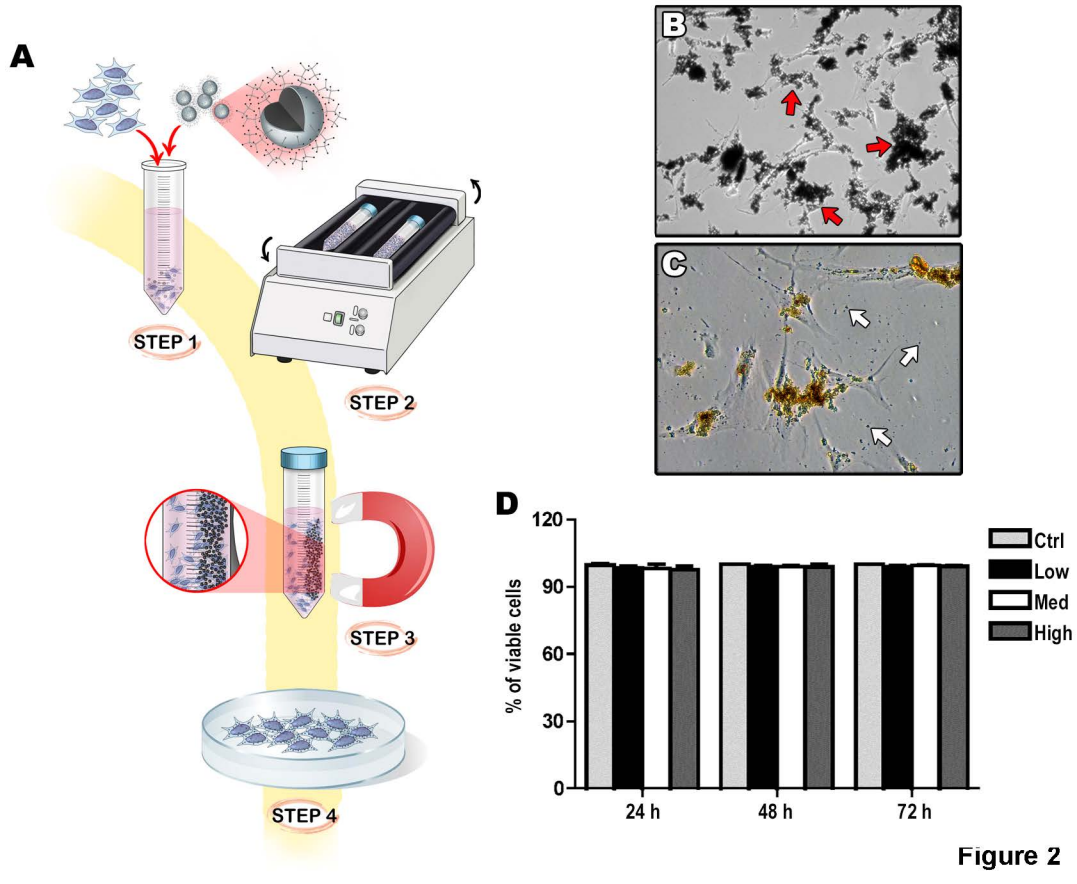
A
STEP 1
STEP 2
STEP 3
STEP 4
B
C
D
% of viable cells
120
90
60
30
0
24 h
48 h
72 h
Ctrl
Low
Med
High

Figure 2

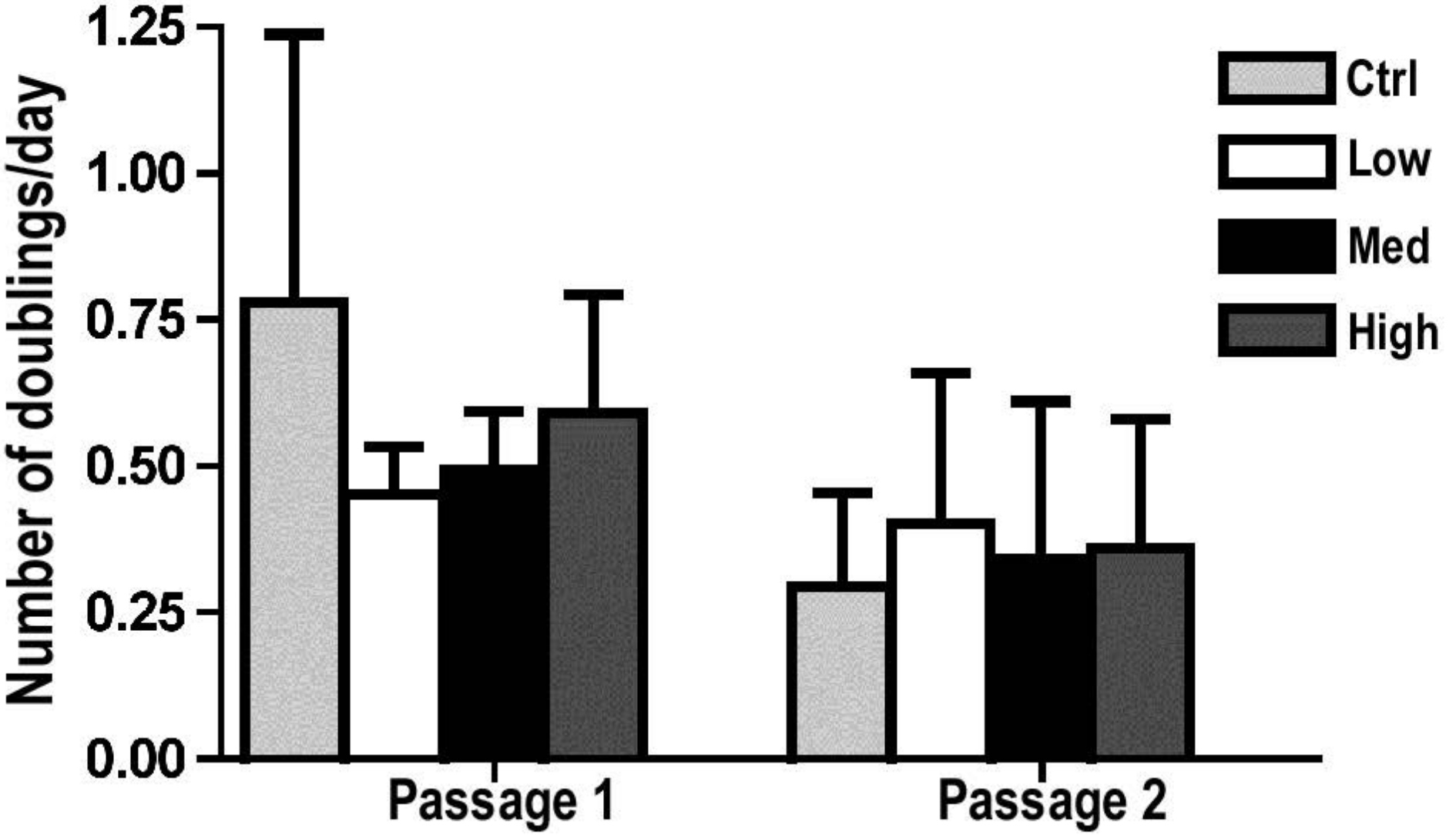
1.25
1.00
0.75
0.50
0.25
0.00
Number of doublings/day
Ctrl
Low
Med
High
Passage 1
Passage 2

Figure 3

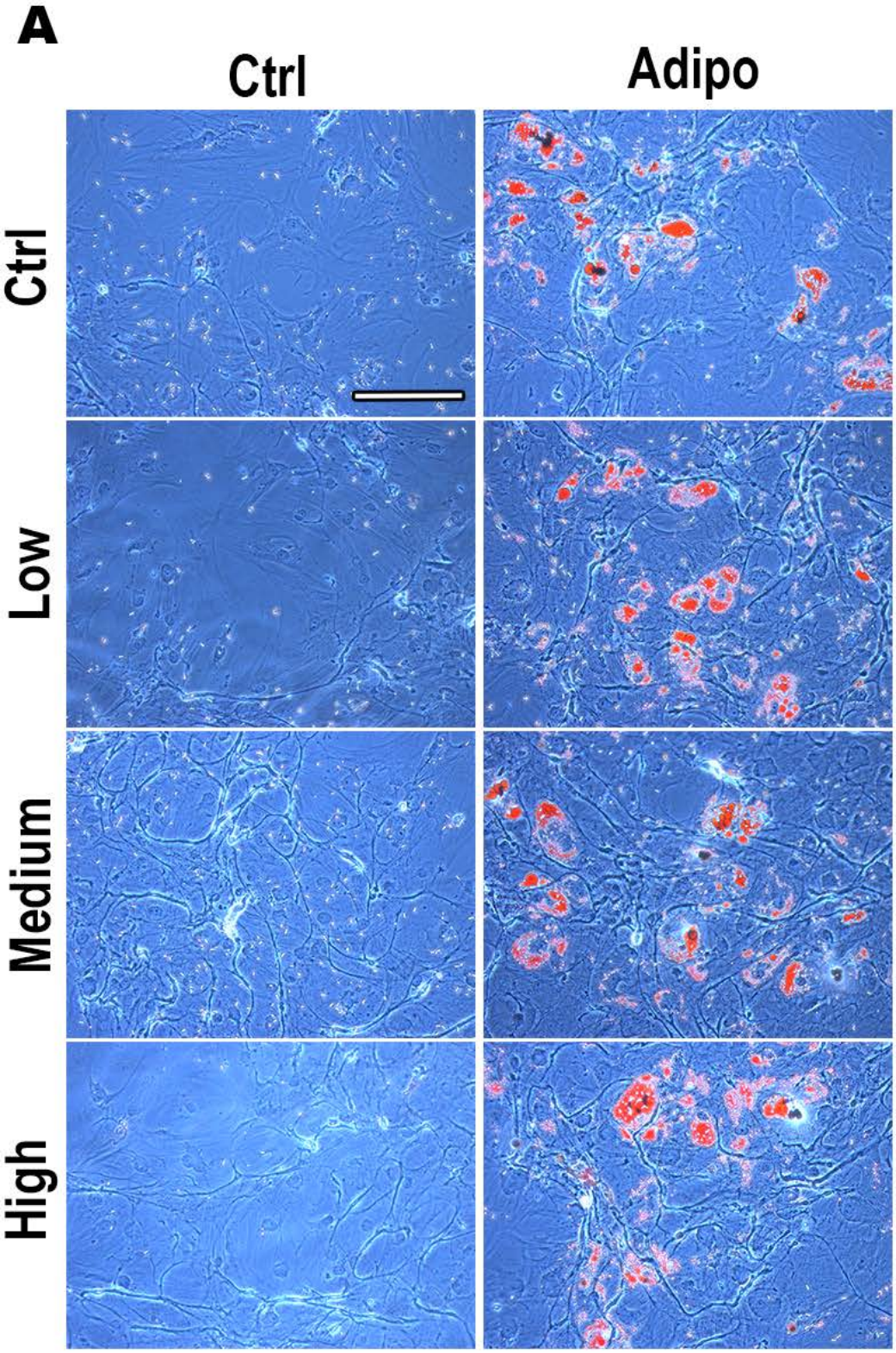
A
Ctrl
Adipo
Ctrl
Low
Medium
High

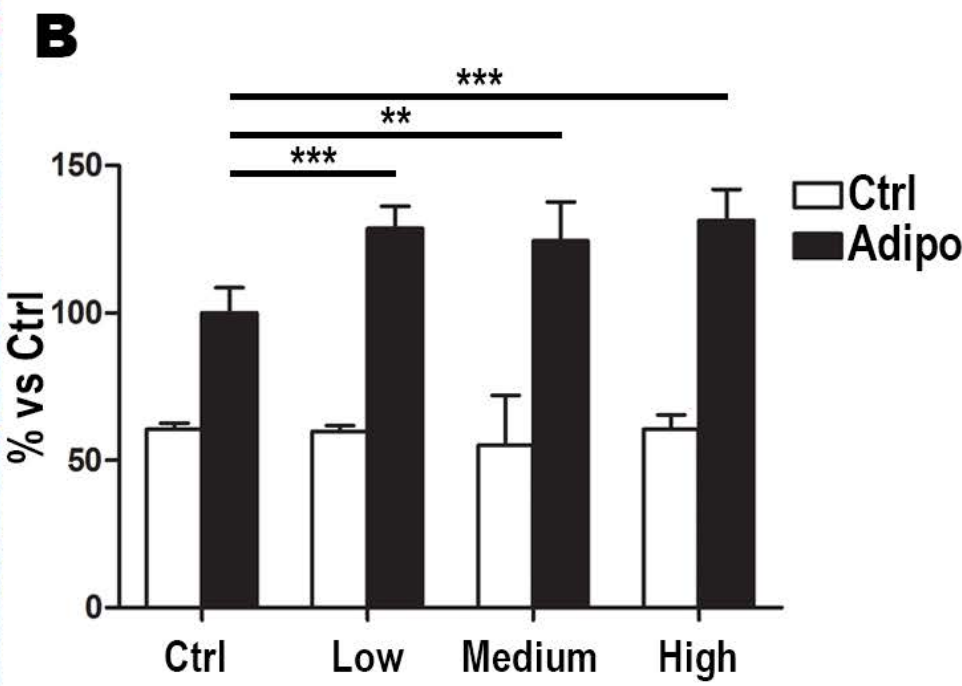
B
***
**
***
150
100
50
0
% vs Ctrl
Ctrl
Adipo
Ctrl
Low
Medium
High

Figure 4

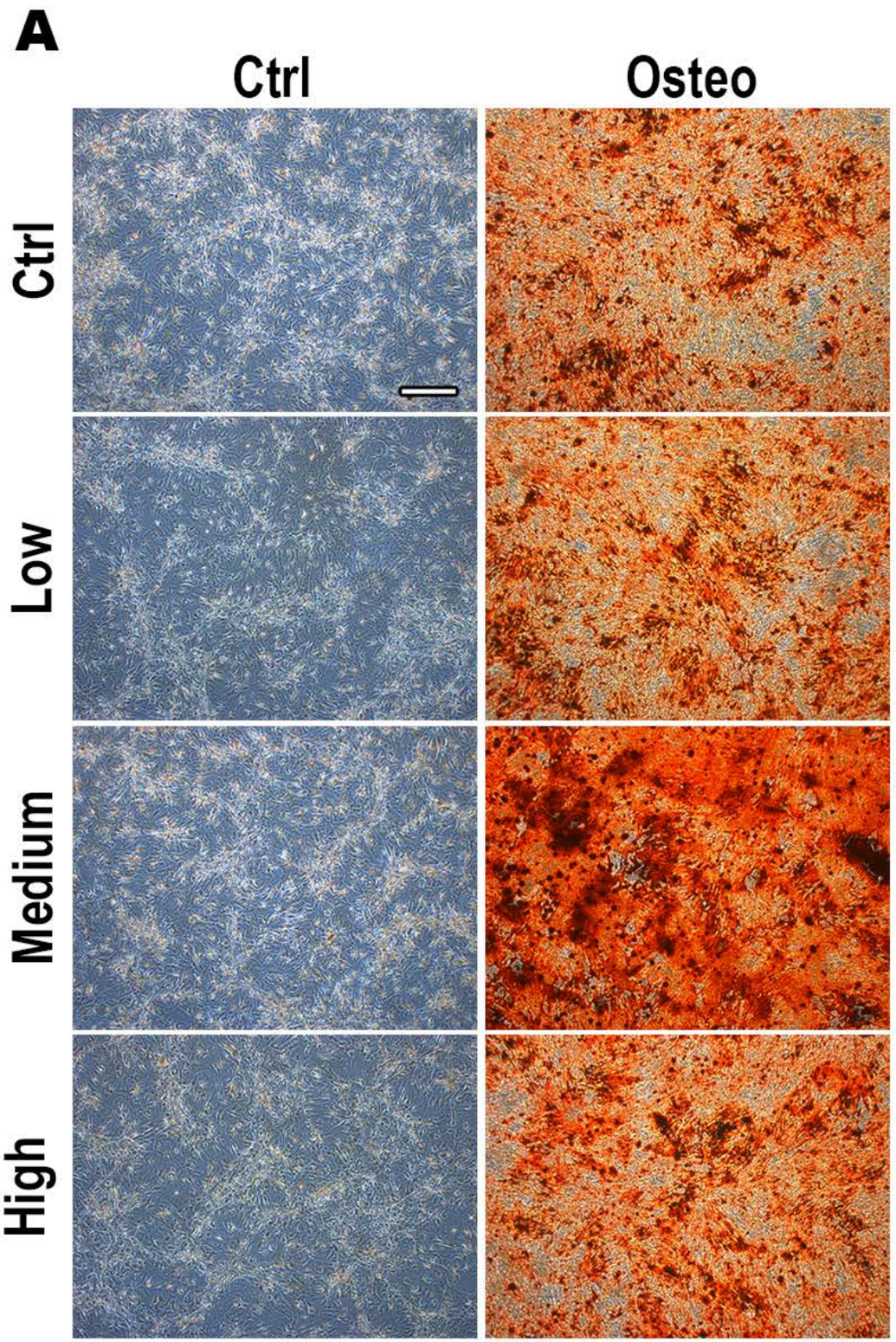
A
Ctrl
Osteo
Ctrl
Low
Medium
High

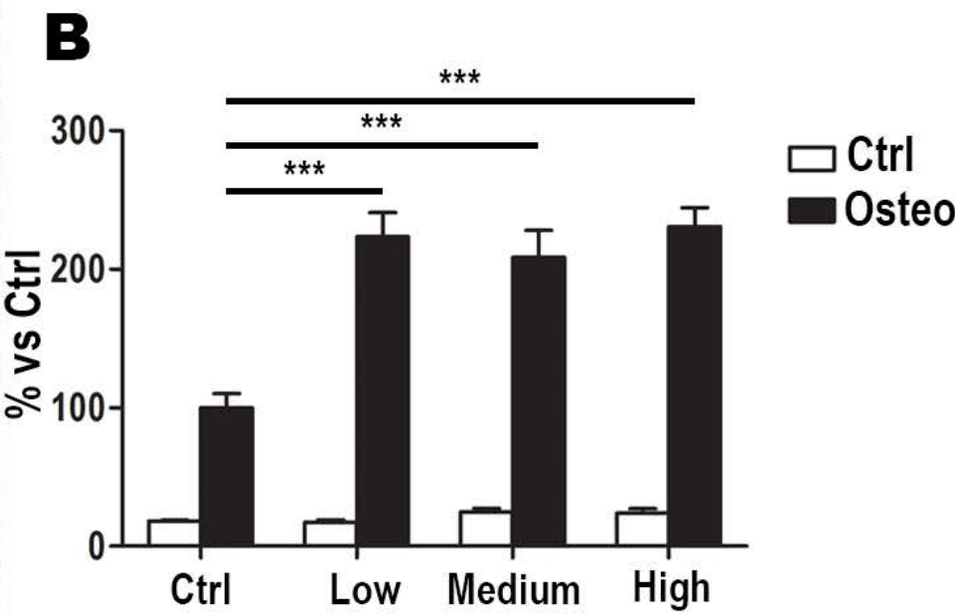
B
***
***
***
300
200
100
0
% vs Ctrl
Ctrl
Osteo
Ctrl
Low
Medium
High

Figure 5

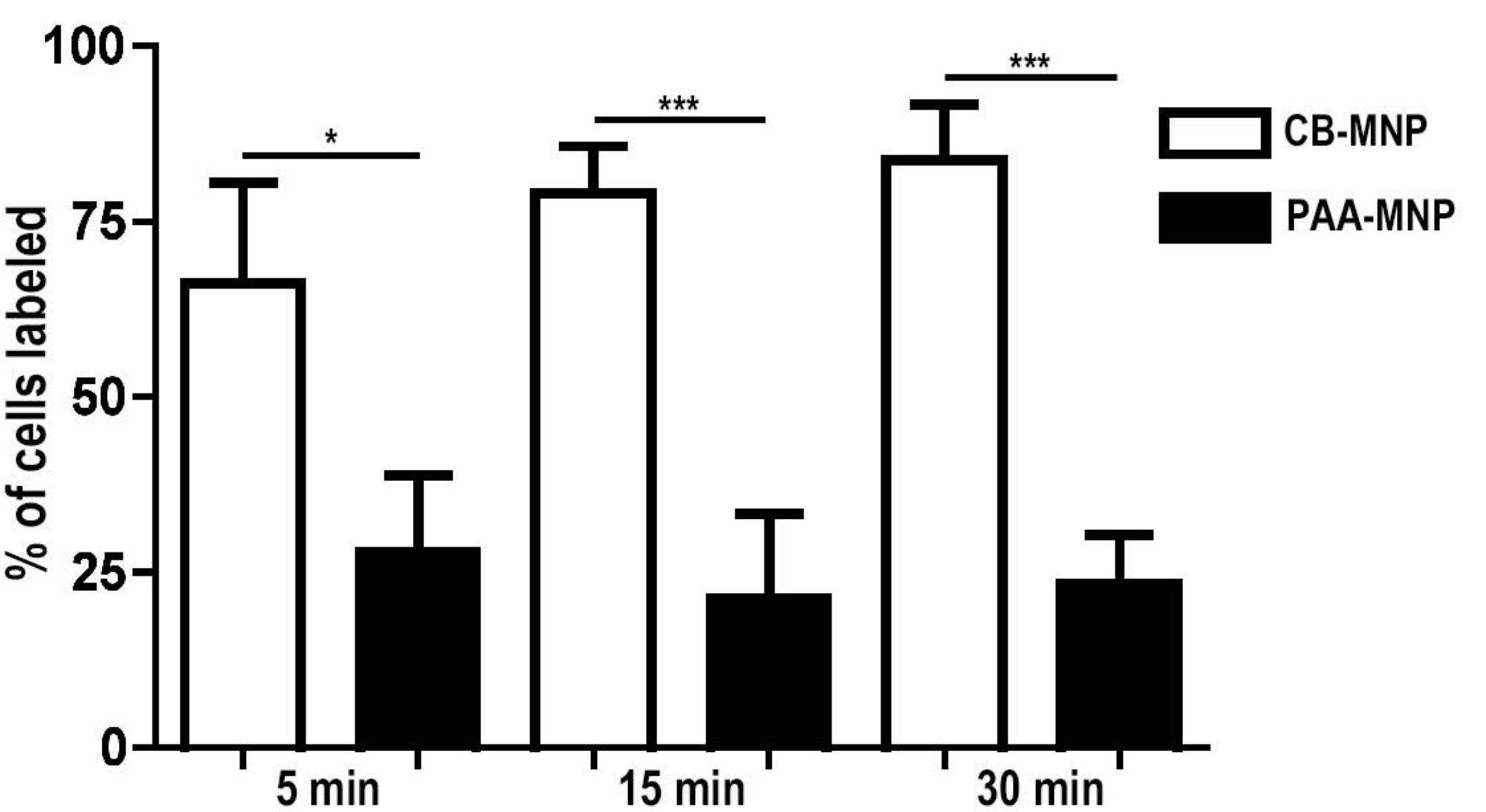

Figure 6

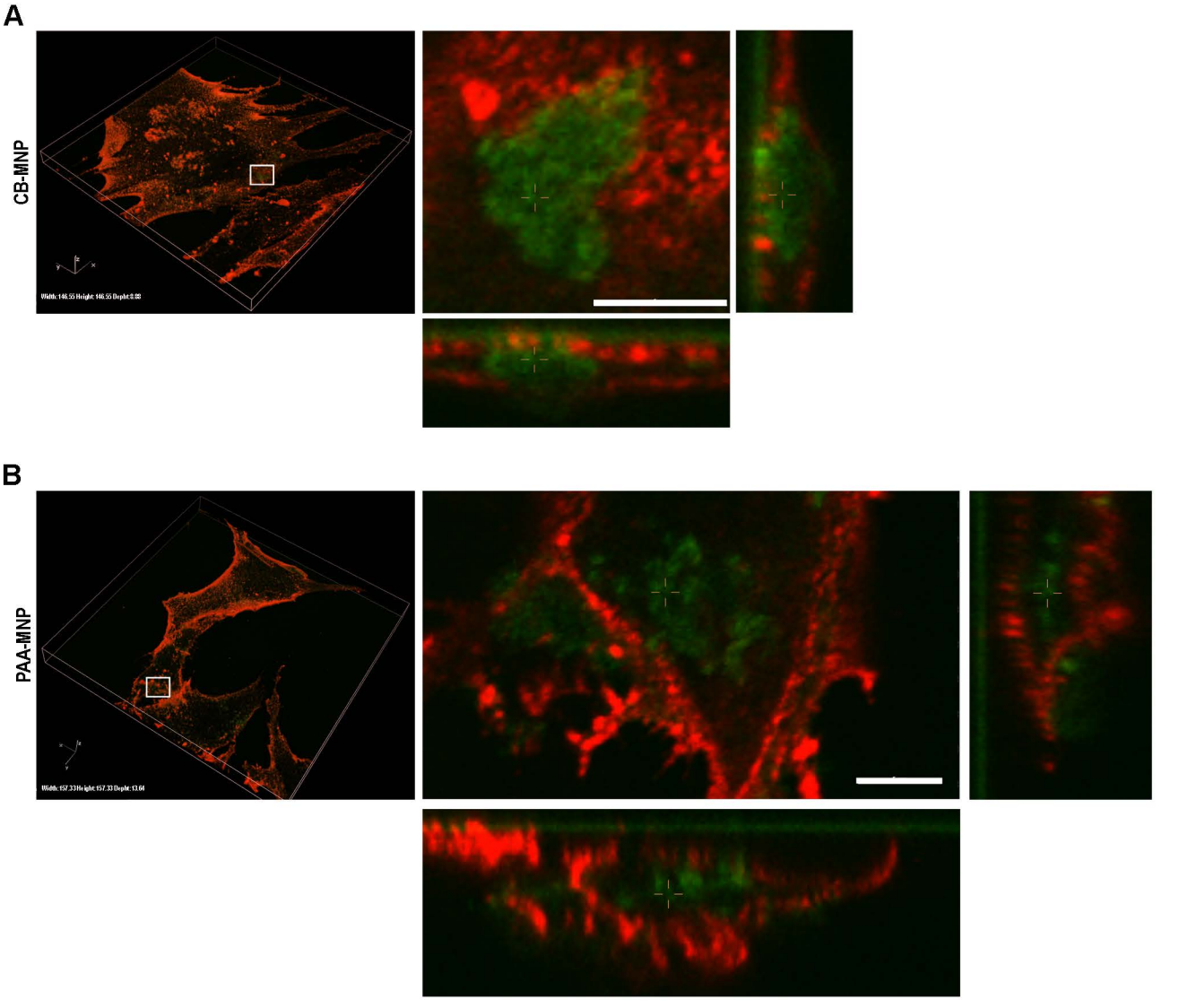

Figure 7

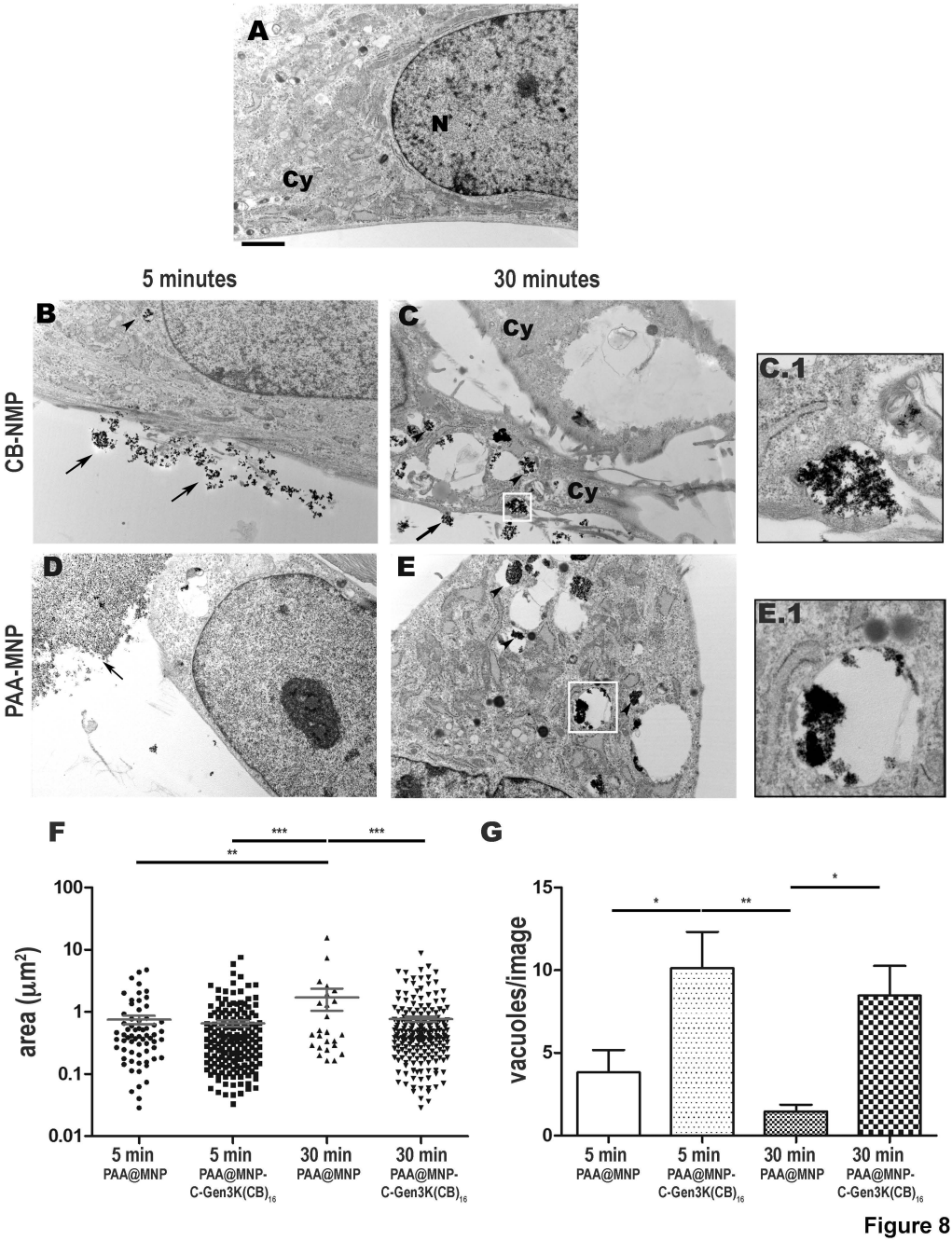
A
N
Cy
5 minutes
30 minutes
B
C
Cy
Cy
C.1
CB-NMP
D
E
E.1
PAA-MNP
F
***
***
**
100
10
1
0.1
0.01
area (µm²)
5 min PAA@MNP
5 min PAA@MNP-C-Gen3K(CB)16
30 min PAA@MNP
30 min PAA@MNP-C-Gen3K(CB)16
G
*
**
*
15
10
5
0
vacuoles/image
5 min PAA@MNP
5 min PAA@MNP-C-Gen3K(CB)16
30 min PAA@MNP
30 min PAA@MNP-C-Gen3K(CB)16

Figure 8